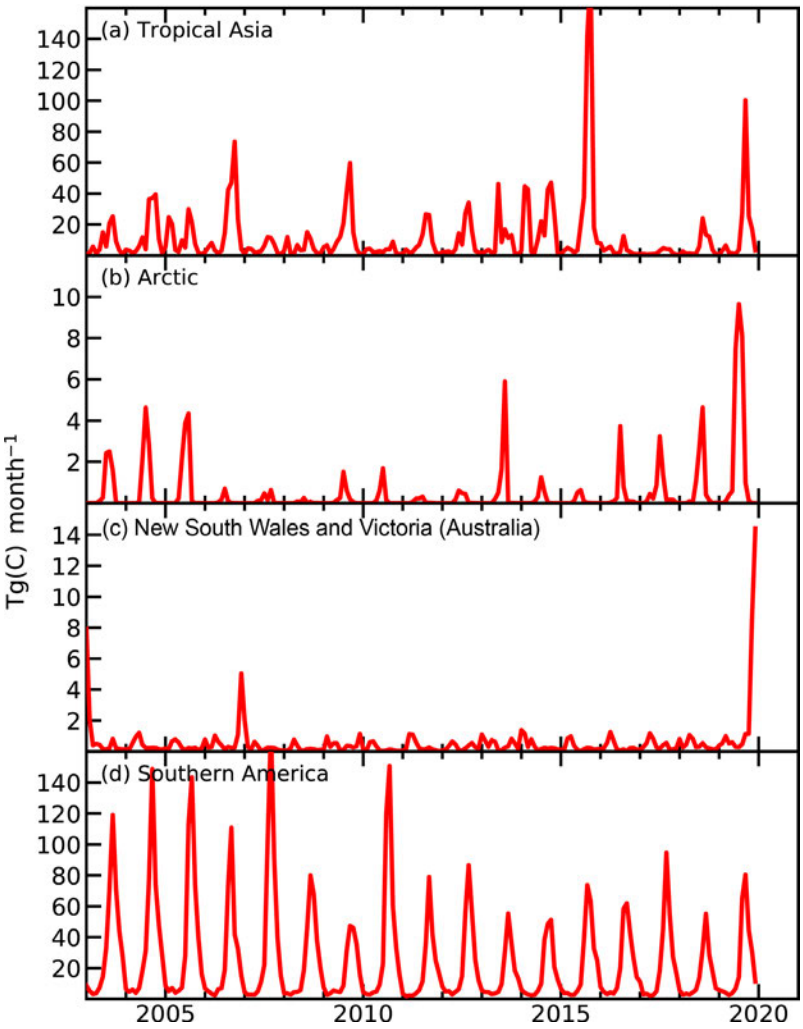

Fig. 2.68. Time series of monthly open biomass burning in (a) tropical Asia, (b) the Arctic, (c) New South Wales and Victoria, Australia, and (d) Southern hemispheric America. The Arctic is bounded by the Arctic Circle (66.5°N); the definitions of the other regions are provided in Table 2.9. (Source: GFASv1.4.)

corresponding reversal of the decreasing long-term trend remains to be seen.

The established long-term downward trend related to changes in land use in frequently burning savannas (Andela et al. 2017), in combination with a delay in the start of the fire season in sub-Saharan Africa, led to a 29% decrease (123 TgC) in fire emissions from NH Africa. Fires here normally burn in December and January but started weeks later related to wet conditions that were associated with the strong positive anomaly of the IOD.

The fire emission estimates have been derived from the Global Fire Assimilation System (GFAS; Kaiser et al. 2012, 2017), which uses satellite data of active fire detections and its intensity and is calibrated against the Global Fire Emissions Database (van der Werf et al. 2017). Here, vegetation fire activity is reported in terms of carbon emissions. Most biomass is released as CO_2, but substantial amounts of other gases and aerosols are emitted as well. Most of the carbon released into the atmosphere is taken up again by vegetation regrowth. However, tropical rain forests and peat lost to fires regrow on time scales longer than a few hundred years or not at all. Their emissions are, therefore, practically irreversible. Given the large spatio-temporal variability in fire activity and the difficulty to constrain those with ground measurements, emission estimates are notoriously uncertain. The presented estimates of relative anomalies in entire regions are more reliable because they are derived from consistent observations by NASA's two satellite-based MODIS instruments. The launch dates of the satellites carrying these instruments restrict the GFAS dataset to the period starting in 2003.

4) Phenology of primary producers—D. L. Hemming, J. Garforth, T. Park, A. D. Richardson, T. Rutishäuser, T. H. Sparks, S. J. Thackeray, and R. Myneni

Climate and nature are mutually dependent. This is visible from global to organism scales by phenological indicators—events in nature (Demarée and Rutishäuser 2011). Here, the timing of NH spring and autumn events of primary producers (terrestrial vegetation and lake plankton) is compared, utilizing records that reach across spatial scales from satellite remote sensing to site-level monitoring.

For 2019, the satellite-derived (MODIS) normalized difference vegetation index (NDVI; Park et al. 2016) revealed the earliest average start of season since the beginning of the record in 2000 (SOSM, 4.3 days) and a later-than-average end of season (EOSM , 2.4 days) across the NH (>30°N),

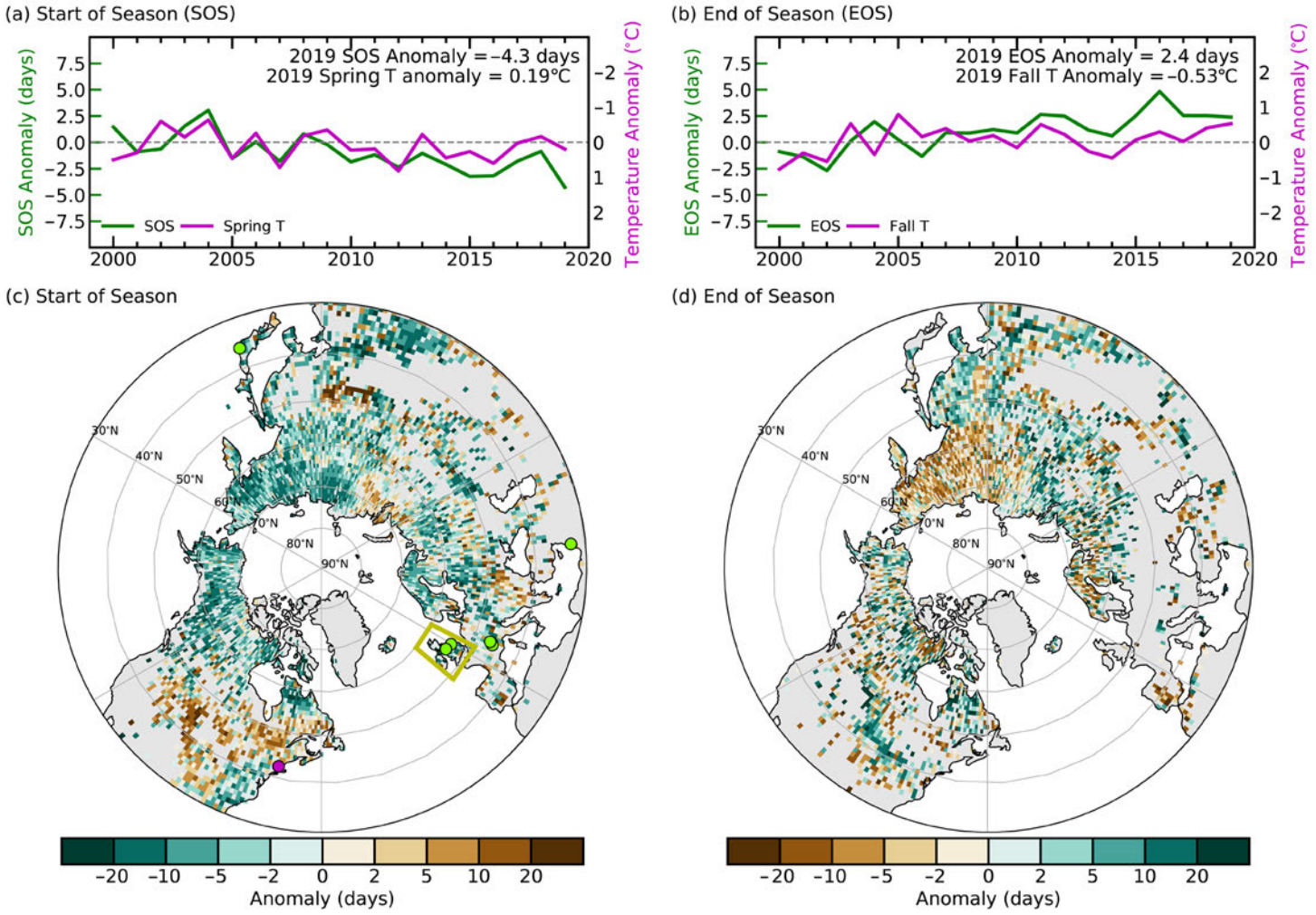

Fig. 2.69. (a) Time series of area mean anomalies (days relative to 2000–09 baseline) in MODIS NDVI-based vegetation growing season onset (SOS; purple) and MERRA-2 spring (Mar–May, green) temperature for NH (> 30°N). (b) Same as (a) but for end of growing season (EOS) and autumn (Sep–Nov) temperature. Note temperature scale reversal in panel (b). Spatial pattern of (c) SOS and (d) EOS anomaly in 2019 with respect to the baseline. Note the color bar reversal in (d) to highlight the longer growing season as green. Colored circles and box in (c) identify the location of sites shown in Figs. 2.70 and 2.71: Harvard Forest PhenoCam site (pink circle), UK phenology network (yellow box), lake phytoplankton NH monitoring sites (green circles).

relative to the 2000–09 baseline (SOS = day of year [DOY] 137, 17 May; and EOS = DOY 283, 10 October; Figs. 2.69a,b). This resulted in an 8-day longer growing season, relative to the baseline (161 days, estimated for all NH pixels and averaged over the baseline). Overall, about 65% and 56% of the NH region showed earlier SOS_M and later EOS_M in 2019, respectively (Figs. 2.69c,d). Regionally, earlier SOS_M occurred across northwestern North America (NA) and most of Eurasia, and later SOS_M occurred over central and eastern NA. A contrasting pattern of earlier and later EOS_M was observed in eastern and western Eurasia, whereas EOS_M in NA was spatially heterogeneous. Interannual variations in SOS_M and EOS_M correlate with changes in spring and autumn temperatures from MERRA-2 reanalysis (Gelaro et al. 2017). For 2019, SOSM and EOS_M are broadly consistent with spatial temperature patterns noted in section 2b of this report.

Two case studies for ground-based phenology observations are compared with the satellite data. PhenoCam data across NA (Richardson et al. 2018a) show similar spatial and temporal patterns to satellite-derived phenology data (Zhang et al. 2018; Richardson et al. 2018b), although the agreement tends to be better in spring than autumn (Melaas et al. 2016; Moon et al. 2019). Here, we compare site PhenoCam estimates for start of season (SOS_{PC}) and end of season (EOS_{PC})

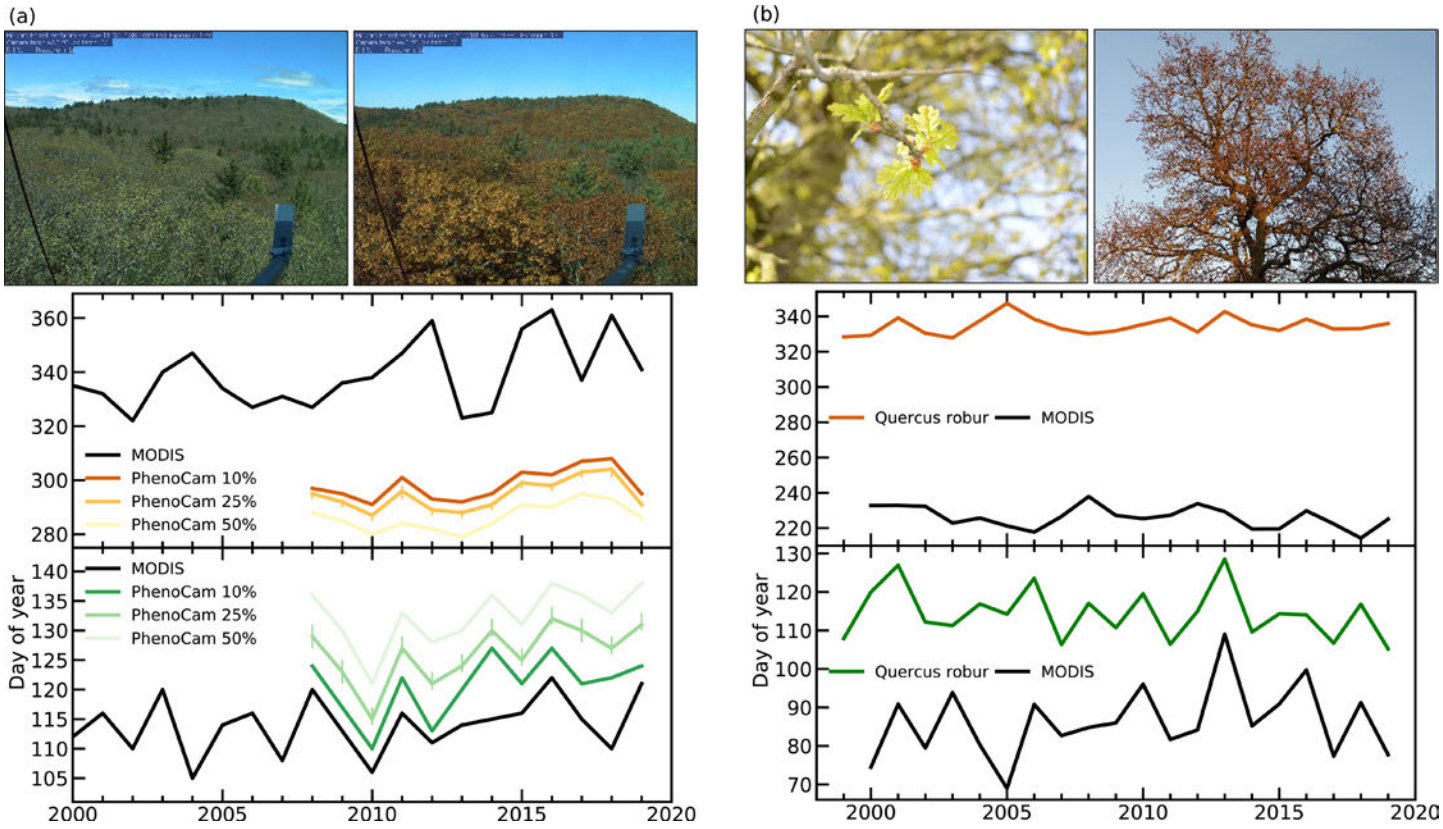

Fig. 2.70. Day of year (DOY) of spring and autumn vegetation phenology indicators and associated 2019 images for (a) Harvard Forest, Massachusetts, United States, SOS (green, bottom) and EOS (orange, top) days derived from PhenoCam and MODIS remote sensing (black), and (b) UK mean oak (*Quercus robur*) "first leaf" (bottom, green), "bare tree" (top, orange), and MODIS (black).

at Harvard Forest, a deciduous forest in Massachusetts (United States) with the same indicators derived from MODIS (Figs. 2.70a,b). SOS_{PC} and SOS_{M} are strongly correlated (r = 0.83, n = 12), although SOSPC is later by 11 ± 3 days, relative to SOS_{M} (Fig. 2.70a). The correlation between EOS_{PC} and EOS_{M} is weaker (r = 0.46), and EOS_{PC} is 48 ± 12 days earlier on average relative to EOS_{M} (Fig. 2.70b). In 2019, SOS_{PC} for Harvard Forest (DOY 131, 11 May, ± 2 days) was four days later relative to 2018 (DOY 127, 7 May, ± 2 days), and EOS_{PC} (DOY 291, 18 October, ± 1 days) was 13 days earlier relative to 2018 (DOY 304, 31 October, ± 2 days). The MODIS changes for this site were more extreme: SOS_{M} was 11 days later and EOS_{M} 20 days earlier in 2019 relative to 2018 (Figs. 2.70a,b). PhenoCam-derived total growing season length in 2019 was more than two weeks shorter than 2018, mostly because of the earlier EOS. This is the shortest growing season observed at Harvard Forest in the 12-year PhenoCam record.

Across the United Kingdom (UK), mean dates of oak (*Quercus robur*) "first leaf" and "bare tree" (indicators of start and end of season) recorded by citizen scientists have been collated by the Woodland Trust since 1999. Over the 2000–09 baseline, the mean first leaf and bare tree dates were 26 April (DOY 116) and 30 November (DOY 334), respectively, giving a 218-day season length (Figs. 2.70b). Both events are strongly influenced by prevailing temperature; first leaf advances by about six days for every 1°C increase in mean February–April temperature, and bare tree dates are delayed by about three days for every 1°C increase in October temperature. In 2019, the very warm spring resulted in mean first leaf nearly 11 days earlier than the baseline. In contrast, October temperature was similar to recent years and bare dates were delayed by about one day compared to the baseline. The net result was an "oak season" 12 days longer than the 10-year mean. These results are qualitatively comparable with UK mean MODIS NDVI SOS and EOS anomalies.

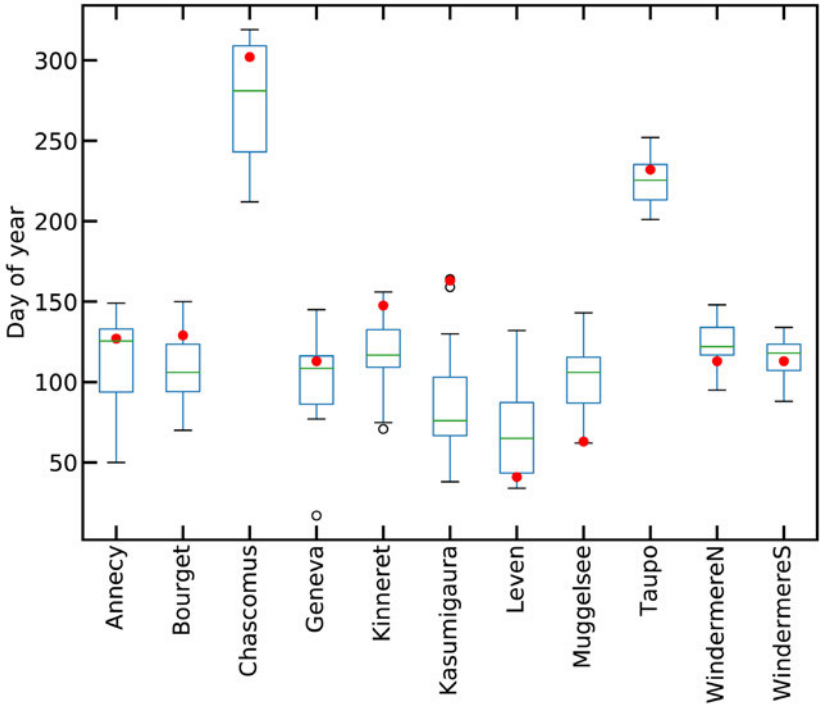

Fig. 2.71. Box-whisker plot showing the DOY of mean (green line), 50th (box), 90th (whiskers), and 99th (black open circles) percentiles of spring phytoplankton peak for 2000–10, and the 2019 mean day (red circles) for nine global lake basins: Annecy and Bourget (France), Chascomus (Argentina), Geneva (France-Switzerland), Kinneret (Israel), Kasumigaura (Japan), Loch Leven (UK), Muggelsee (Germany), Taupo (New Zealand), and Windermere north and south basins (UK).

Long-term (fortnightly-monthly) monitoring data on lake water concentrations of the photosynthetic pigment chlorophyll-*a* can be used to derive the seasonality of phytoplankton growth and the timing of the spring phytoplankton peak in lake ecosystems (Winder and Cloern 2010; Thackeray et al. 2013). We present such data from 11 lake basins (Fig. 2.71): Lakes Annecy and Bourget (France), Chascomus (Argentina), Geneva (France-Switzerland), Kinneret (Israel), Kasumigaura (Japan), Loch Leven (UK), Müggelsee (Germany), Taupo (New Zealand), and the north and south basins of Windermere (UK). During the 2000–10 baseline, the mean day of year of the spring bloom in the nine NH basins ranged from 76 (17 March, Loch Leven) to 122 (2 May, Windermere North Basin). In lakes Chascomus and Taupo, in the SH, the corresponding means were 274 (1 October) and 222 (10 August), respectively. In 2019, the day of year of the spring peak was later than the base period in eight lake basins (by 1 to 82 days), but earlier for Müggelsee, Loch Leven, and Windermere North Basin (by 37, 35, and 9 days, respectively). This site-based variability suggests the agency of additional factors, such as nutrient availability (Thackeray et al. 2008), that interact with climate to influence seasonal ecosystem behavior.